Enhanced Detection of Hydrogen Peroxide with Platinized Microelectrode Arrays for Analyses of Mitochondria Activities

Salem Ben-Amor, Emilie Vanhove, Fadhila Sekli-Belaidi, Samuel Charlot, David Colin, Michel Rigoulet, Anne Devin, Neso Sojic, Jérôme Launay, Pierre Temple-Boyer, et al.

Enhanced Detection of Hydrogen Peroxide with Platinized Microelectrode Arrays for Analyses of Mitochondria Activities

Salem BEN-AMOR [1,2], Emilie VANHOVE [3,4], Fadhila SÉKLI BELAÏDI [3,4], Samuel CHARLOT[3,4], David COLIN[3,4], Michel RIGOULET[5], Anne DEVIN [5], Neso SOJIC [1,2], Jérôme LAUNAY[3,4], Pierre TEMPLE-BOYER[3,4], Stéphane ARBAULT[1,2]

[1] CNRS-LAAS; 7 avenue du colonel Roche, F-31400 Toulouse, France

[2] Université de Toulouse; UPS; LAAS; F-31400 Toulouse, France

[3] Univ. Bordeaux, ISM, UMR5255, F- 33400 Talence, FRANCE

[4] CNRS, ISM, UMR5255, F- 33400 Talence, FRANCE

[5] University Bordeaux 2, Institute of Cell Biochemistry and Genetics, CNRS UMR 5095, F33077 Bordeaux, France

Corresponding Author: Dr. Stéphane ARBAULT; Address: Univ. Bordeaux, ISM, CNRS UMR 5255, F- 33400 Talence, FRANCE; email: stephane.arbault@enscbp.fr

KEYWORDS: Microelectrode array; platinization; hydrogen peroxide; nanomolar detection; oxidative stress.

ABSTRACT:

Black platinum-modified ultramicroelectrodes (UME) were previously reported as excellent sensors for hydrogen peroxide produced by biological systems; their detection limit being typically 100 nM. In the present work, we took benefit of an ultramicroelectrode array configuration (16 x 20 µm diameter-disk UME) to increase the overall electroactive surface and consequently, faradaic currents. Platinum-UME arrays integrated on a silicon chip were characterized by cyclic voltammetry before and after platinization for ferricyanide reduction and hydrogen peroxide oxidation in comparison with a single platinized UME. Then, UME arrays were platinized at different coulometric charges (0.04 $\mu C.\mu m^{-2}$ to 3.2 $\mu C.\mu m^{-2}$) to determine the best compromise between faradaic and capacitive currents associated with the hydrogen peroxide oxidation wave. Sensitivity and detection limit for H_2O_2 of these different platinized UME arrays were studied by chrono-amperometry at +300 mV vs Ag/AgCl. The detection limit was lowered to 10 nM H_2O_2 in buffer with the UME arrays, which is an excellent condition for biological measurements. Black platinum-modified UME arrays were eventually used to monitor the production of H_2O_2 by mitochondria under a condition favoring the oxidative stress pathway; a flux of few nanomoles H_2O_2/mg protein/min. was detected with kinetic and quantitative accuracy.

1. Introduction

Hydrogen peroxide is widely recognized as a major bioactive molecule produced by aerobic metabolic pathways [1]. H_2O_2 is a key component among the reactive oxygen species family ($^1O_2$, $O_2^{\circ-}$, H_2O_2, OH° ...) since it is a kinetically stable intermediate that will either react itself with, or lead to more reactive species toward the biological architectures (DNA, proteins, lipids). Thus, hydrogen peroxide is considered as a keystone molecule of oxidative stress processes[2, 3] and consequently, is a major target for analytical techniques applied to biology [4, 5].

Hydrogen peroxide has thus attracted over the last two decades much attention from analysts and particularly from electrochemists in order to develop specific detection methods and sensors for this molecule. In the electroanalytical field, many strategies have now been reported for the building of electrode surfaces that confer high selectivity and sensitivity for H_2O_2 [6, 7]. These strategies include mediated or direct transfer to oxidases (peroxidases mostly) decomposing hydrogen peroxide [4, 8, 9], as well as direct oxidation or reduction on different catalytic surfaces [6, 10-12]. More complex architectures have also been proposed recently, mixing e.g. carbon nanotubes or redox polymers, nanoparticles and possibly, enzymes to combine advantages of catalytic activities with high active surface areas of designed electrodes [4, 6, 13-15].

However, platinum still appears as the best catalyst surface for the direct electrochemical oxidation or reduction of hydrogen peroxide, whatever its material shape and dimensions are. In

particular, structured platinum surfaces are mechanically robust and provide fast response-times, which become important features for monitoring H_2O_2 in vivo [7, 16-18]. Among designed micrometric and nanometric platinum surfaces, "Black platinum" electrodes have proven their interest for direct measurements in biological buffers, on cells or in a tissue [16, 17, 19-22]. In addition, they offer an accurate detection over a large range of H_2O_2 concentrations [16, 23, 24]. Their sensitivity and detection limit for H_2O_2 can be adjusted as function of the quantity of platinum electro-deposited, since a rough surface with high active area is obtained [16, 23, 24]. We reported recently [24] that platinized platinum ultramicroelectrodes (20 µm diameter) offer an effective detection limit (measured and not calculated) of 100 nM for H_2O_2 in buffered solutions, and a linear dependence of their current response versus H_2O_2 concentrations ranging from 100 nM to 50 µM, at least. Elsewhere, Li et al reported[25] an even lower detection limit for hydrogen peroxide, i.e. 10 nM, with black platinum-coated platinum band microelectrodes (200 µm width). Though this was obtained under flow in a micro-channel configuration and consequently, in a confined detection volume and not in bulk, it showed that the detection of very low concentrations, below 100 nM, depends both on the increase of active area of the electrode surface and on our experimental ability to measure very low chrono-amperometric currents (pico- to femto-amperes range), due to the micrometric size of our sensors. In this context, micro-band surfaces provide currents much larger than micro-disks, at equivalent platinization charge densities.

Such interest in increasing the surface-area of electrodes, while keeping a micrometric size of one of their dimensions and consequently the specific mass-transport features of microelectrodes, has been extensively described in the literature [26]. A typical geometry to achieve this goal is a

collective array of ultramicroelectrodes, or even nanoelectrodes, connecting tens to hundreds of micrometric to sub-micrometric disks or bands [14, 18, 19, 27-31]. By choosing during fabrication an adequate ratio between the radius of each electrode and the distance between them [27, 28], one may obtain an hemispherical diffusion field at each electrode surface while adding their currents for the whole array and thus detecting large steady-state currents. In the present work, we took benefit of such a configuration of an ultramicroelectrode array (16 x 20 µm-diameter disk UME) and studied, following its platinization, the detection of hydrogen peroxide, in comparison with a single platinized ultramicroelectrode (1 x 20 µm-diameter). Black-platinum modified ultramicroelectrode arrays were characterized by voltammetry and chrono-amperometry for the electro-oxidation of H_2O_2 as function of the platinization coulometric charge. The array-configuration allowed decreasing the degree of platinization compared to a single ultramicroelectrode, leading to lower capacitive currents and increased faradaic currents and providing higher signal-to-noise ratios. The detection-limit for H_2O_2 of these microsensor arrays reached 10 nM, which is a major feature for the monitoring of hydrogen peroxide in biological conditions. An example of biological measurement is presented consisting in the detection of hydrogen peroxide produced by mitochondria *in vitro*.

2. Experimental

2.1. Fabrication of the ultramicroelectrode arrays

Platinum ultramicroelectrode arrays were fabricated using silicon-based technologies [32]. Starting from an oxidized silicon wafer (oxide thickness: 600 nm), different thin–film layers were evaporated under vacuum in conventional physical vapour deposition (PVD) equipment,

and patterned using a classical “lift-off” technique. Two PVD processes were performed in a row: a 120 nm platinum layer was deposited on a 12 nm titanium underlayer in order to ensure platinum adhesion on silicon oxide. These thicknesses values were chosen in order to enhance adhesion properties while limiting technological defects related to mechanical stress and inter-diffusion phenomena of metallic atoms (Ti, Pt, and Ag). Finally, microdevices were passivated by depositing by ICP-CVD (inductively-coupled plasma chemical vapour deposition) at low temperature (100°C) an inorganic silicon nitride SiN_x film (thickness: 110 nm) on the whole wafer except for the microelectrode (working and counter-electrodes) active areas as well as for the contact pads [33]. This last patterning was performed using a bilayer "lift-off" technique [33]. This wafer-level passivation process was used to insulate electrically the different metallic layers, to define precisely the different electrochemical active surfaces and insure an improved life-time compared to standard organic passivation layers [33]. The platinum working ultramicroelectrode arrays were defined as arrays of disk-shaped electrodes, which individual geometric surface was 315 μm^2 (radius: 10 µm). Platinum counter microelectrodes were integrated as a band electrodes (~ 0.135 mm^2) surrounding the working UME array. All in all, four independent UME arrays were realized on each silicon chip (Fig. 1).

After dicing, chips were then reported and glued on a specific, back-side connected, printed circuit board. Special care was brought about the packaging and wiring processes in order to realize "pencil-like" electrochemical microsensors and to finally ensure the compatibility of the fabricated microsystems with analysis into an oxygraphy chamber for studies of mitochondrial activities.

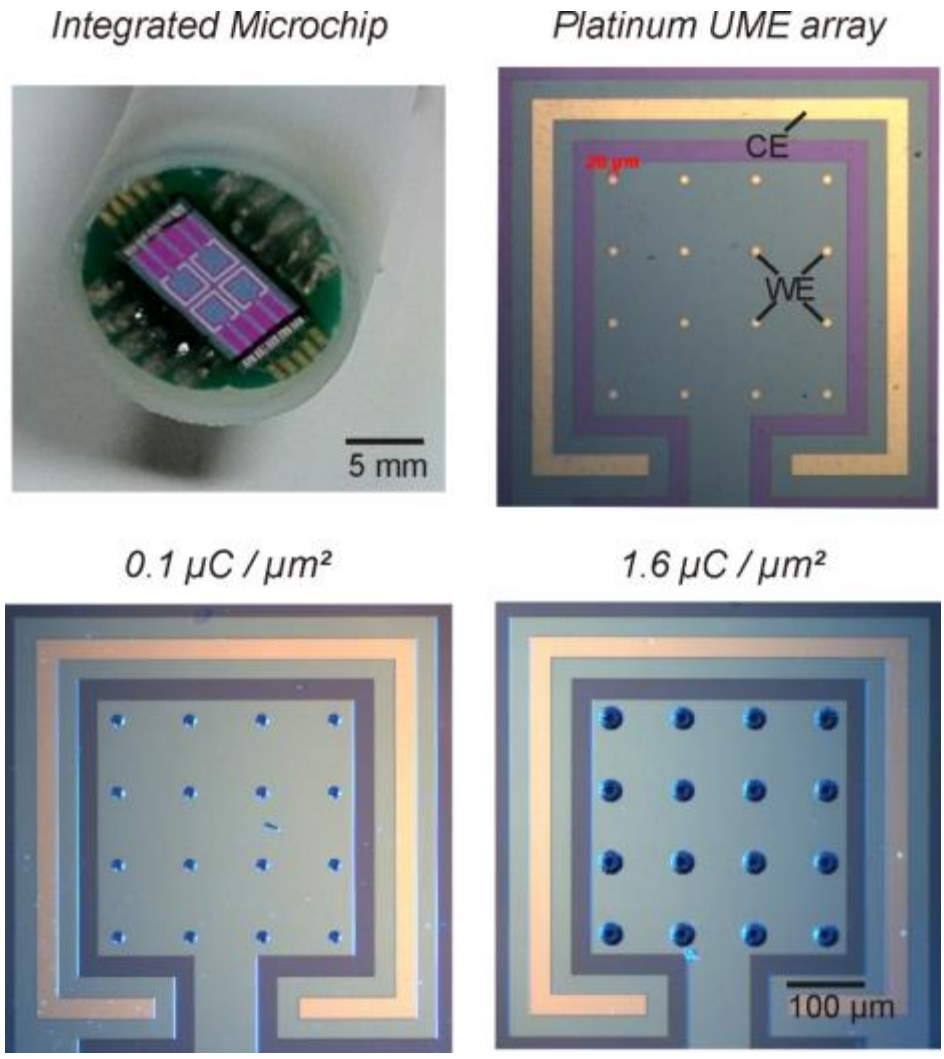

Fig. 1. Microtechnological integration of ultramicroelectrode arrays on a silicon chip. Each chip (top left) includes four arrays of platinum ultramicroelectrodes (16 UME of 20 µm diameter each; individual geometric surface area ~ 315 µm^2; top right) and four associated-platinum counter microelectrodes (band electrodes of *circa* 0.135 mm^2 geometric surface area). Electrochemical responses of the ultramicroelectrode arrays have been characterized before and after their electro-platinization at different coulometric charges; two typical degrees of platinization are shown on the images in low position.

2.2. Electrodeposition of black-platinum and surface treatment

Black-platinum deposit on ultramicroelectrodes' surface, i.e. the platinization process, was achieved by reducing hydrogen hexachloroplatinate (31.2 mM in PBS) in the presence of lead acetate (0.67 mM) at -60 mV versus Ag/AgCl/KCl 3.5 M. The linear increase of the reductive deposition current was followed along the time and the process was interrupted when the coulometric charge reached different desired values: 0.04; 0.1; 0.3; 1.6 and 3.2 $\mu C.\mu m^{-2}$. Platinized ultramicroelectrode arrays were rinsed several times with distilled water and exposed just before use to an oxygen plasma within a so-called plasma cleaner (Harrick Plasma inc., plasma-Flow PDC-FMG). The exposure chamber was previously cleaned with acetone and isopropanol. After inserting the sample, chamber was subjected to vacuum in order to reach a 75 mTorr pressure in situ. 100 % oxygen flow was then injected in the cell to have a pressure of 1250 mTorr. After 20 min. exposure at maximum power (30 mW), the sample was removed and immediately soaked in PBS pH 7.4. All chemicals were from Sigma-Aldrich inc., except when noticed.

2.3. Electrochemical measurements

The electrochemical measurements were carried out using a potentiostat (BioLogic inc. VSP-300, EC-Lab software) equiped with an ultralow current module (sub-picoampere residual rms noise at 1 nA scale factor). An Ag/AgCl/KCl 3.5 M electrode or a Ag/AgCl wire (freshly chlorinated) were used as reference electrode. Electrochemical experiments were performed either in a standard single compartment electrochemical cell for voltammetric experiments, either in a 28°C-thermostated oxygraphy chamber under constant stirring (800 rpm) for chrono-amperometric measurements. 6 µL of concentrated H_2O_2 solutions were injected in the 6 mL-

volume of the chamber, so as to obtain final concentration variations of 10 nM, 100 nM, 1 µM and 10 µM H_2O_2. Electrochemical experiments were carried out in PBS buffer (10 mM phosphates, 138 mM NaCl, 2.7 mM KCl). Cyclic voltammograms (CVs) were conducted at 20 $mV.s^{-1}$ scan rate between +250 mV and -50 mV, or +50 mV and +350 mV vs. Ag/AgCl for ferricyanide and hydrogen peroxide solutions, respectively. Chrono-amperograms were obtained by setting the working electrode potential at +300 mV vs. Ag/AgCl and waiting for current stabilization (drift below 10 % over 10 min. duration) before measurement.

2.4. Mitochondria preparation

Mitochondria were extracted from yeasts (*Saccharomyces cerevisiae,* strain BY 4742). Cells were grown aerobically at 28°C in a pH 5.5 medium containing 0.175% yeast nitrogen base (Difco), 0.2% casein hydrolysate (Merck), 0.5% $(NH_4)_2SO_4$, 0.1% KH_2PO_4, 2% lactate(w/v) (Prolabo) as carbon source, 20mg/L L-tryptophan, 40mg/L adenine hydrochloride and 20mg/mL uracil. Cells were harvested in the exponential growth phase, and mitochondria were isolated from protoplasts, as described previously [34]. Mitochondrial protein concentration was measured by the Biuret method using bovine serum albumin as a standard. Mitochondria were suspended and analyzed in a specific medium, so-called Mitochondrial Buffer (MB) containing 0.63M de-ionized mannitol, 0.36 mM EGTA, 10 mM Tris-maleate, 5 mM Tris-phosphate, adjusted at pH 6.8. In order to measure solely the H_2O_2 production by the respiratory chain, endogenous catalase activity mitochondria was inhibited by incubating them before measurement with 0.5 mM KCN in MB at 4°C for 20 min [35]. The suspension was then centrifuged twice at 8000 g and 4°C for 10 min, the supernatant being each time removed and mitochondria being suspended in a few µL of MB. Finally, prepared mitochondria samples could be directly injected

in the oxygraphy chamber, subsequently followed by injection of ethanol (1% final concentration) and antimycin A (0.5 µM).

3. Results and Discussion

3.1. Electrochemical characterization of the platinum-ultramicroelectrode array based on ferricyanide reduction

Platinum disk-shaped ultramicroelectrode arrays (16 x 20µm-diameter electrodes) were fabricated as described above based on platinum-thin film sputtering and photolithography on a silicon chip (Fig. 1). Their electrochemical responses were characterized before and after platinization, in comparison with single platinum ultramicroelectrodes of the same diameter, i.e. 20 µm. Characterization was based on cyclic voltammetry responses of the two ultramicroelectrode configurations for the reduction of a standard outer-sphere redox couple ($Fe(CN)_6^{3-}/Fe(CN)_6^{4-}$) and for the oxidation of the product of interest in this study: hydrogen peroxide.

We had first to check out that the "thin film" platinum layers of the arrays provided electrochemical features similar to native solid surfaces obtained from a polished section of a micrometric wire. Ferricyanide reduction is commonly used to assess differences in electrochemical behaviour of surfaces, because of the molecule sensitivity to adsorptive specific sites accompanying its electro-reduction. As shown in Fig. 2, platinum UME arrays displayed similar steady-state voltammetric responses, in terms of $Fe(CN)_6^{3-}$ reduction potential and kinetics, than a single solid UME. The array provided typical sigmoidal-shaped voltammograms for steady-state responses, showing that the ratio of “distance between UME/radius of each

UME", which equals 10 herein, was adequate to create an individual hemi-spherical diffusion field at each UME [27, 28]. Obviously, plateau currents detected with the array, i.e. 140 nA, were higher than the plateau current for a single 20 µm-diameter UME, i.e. 9 nA; the ratio (15.5) between these currents corresponding well to the increase of ultramicroelectrodes' number, 16 on our device, and overall active surface.

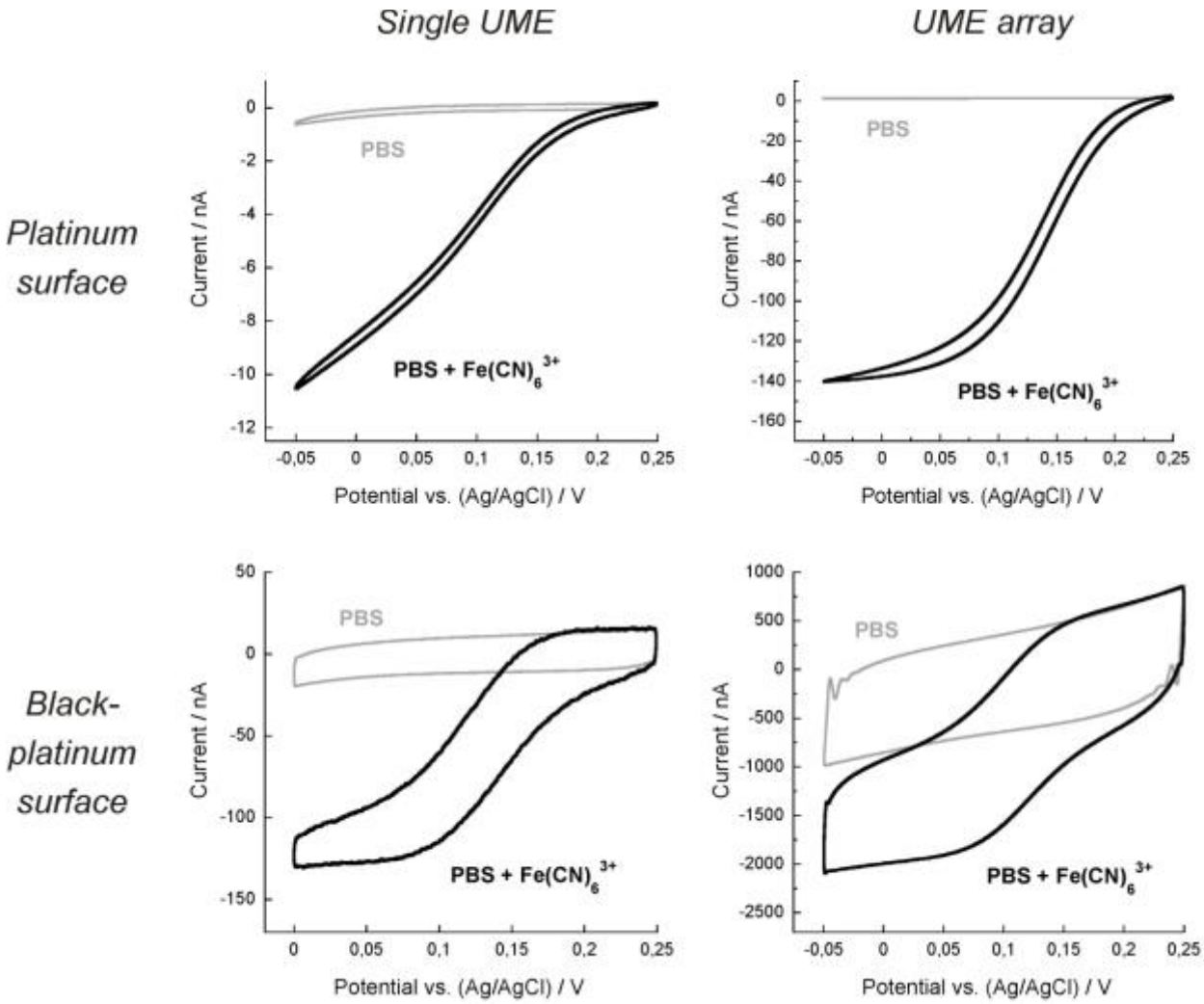

Fig. 2. Comparison of voltammetric responses (20 $mV.s^{-1}$) from a single platinum ultramicroelectrode (20µm-diameter obtained from a polished section of a platinum wire) and a silicon-based, integrated ultramicroelectrode array (16 x 20 µm-diameter), before and after

platinization (3.2 $\mu C.\mu m^{-2}$ for each), for the reduction of ferricyanide (5 mM $Fe(CN)_6^{3-}$ solution in PBS).

3.2. Platinization of the ultramicroelectrode array for the electro-oxidation of hydrogen peroxide

The next step consisted in modifying the surface of ultramicroelectrode arrays by black platinum deposits. We and others [17, 21, 24, 36] have demonstrated the interest of such platinum surfaces with meso to nanoscale intimate structuration to increase the active surface area of ultramicroelectrodes. In addition, black platinum deposits are achieved under full electrochemical control, i.e. the coulometric charge electro-deposited, so as to adjust the electrode sensitivity. In addition, it was shown for decades that the change of chemical state of the black-platinum surface in comparison with polycrystalline surfaces from solid platinum wires, might provide a high catalytic activity [24],[25, 37, 38]. This was usually favorable to increase charge transfer rates and to analyze species hardly detectable either by oxidation or reduction. This is typically the case for the reduction of ferricyanide or the oxidation of hydrogen peroxide (Fig. 2).

As observed for single platinized ultramicroelectrodes, the voltammetric reduction of ferricyanide appears better defined with a sigmoidal-shaped curve when detected at a platinized UME array (Fig. 2 bottom part) than at the bare platinum surface. Faradaic as well as capacitive currents were largely increased following platinization of the array. Black-platinum surfaces indeed possess high capacitive charges inducing high background capacitive currents in voltammetry and often, non-stable slowly discharging currents in chrono-amperometry.

However, the faradaic current detected with the platinized array was sufficiently increased to reach the micro-ampere range in voltammetry. Similarly to non-modified surfaces, the ratio of plateau currents for the reduction wave of ferricyanide was about 12-fold between a single platinized UME and the UME array platinized at the same coulometric charge density (3.2 $\mu C.\mu m^{-2}$ in Fig. 2). Besides, comparison were achieved following a pre-treatment by an oxygen-plasma (see experimental section) of all electrode types, since we demonstrated [24] that this physical surface-treatment decreased the capacitive currents of black-platinum surfaces and improved their sensitivity. An exactly similar improvement of platinized surface electrochemical activity, leading to an increase of Signal/Noise by 3 to 5-fold, was observed herein for the modified UME arrays such like for single UMEs (data not shown).

Then, platinized UME arrays were analyzed for the oxidation of hydrogen peroxide solutions in a PBS buffer (Fig. 3). Again, similarly with single platinized UME, platinized arrays provided sigmoidal-shape waves (at 20 $mV.s^{-1}$ scan rate and below) for H_2O_2 oxidation corresponding to a quasi-steady state response in voltammetry. The plateau potential of the oxidation wave, used for further chrono-amperometric measurements (see 3.3.), was calculated as +300 mV vs. Ag/AgCl, i.e. at a potential much lower than for non-platinized surfaces e.g. +600 mV [24]. Nevertheless, voltammograms obtained with UME array displayed large capacitive currents that might lead to very slowly discharging currents in chrono-amperometry (see below 3.3.).

We studied the effect of the black-platinum electro-deposition level on the features of voltammograms for H_2O_2 oxidation (Fig. 3). Arrays were platinized at five different charges, which corresponded not only to different electrochemical responses but also to physical

differences of the deposits, as shown on the images of Fig. 1. Indeed, black-platinum deposits at coulometric charges from 0.1 to 0.3 $\mu C.\mu m^{-2}$ were rather small in size, not really changing the diameter of each UME on the array, while deposits obtained at values higher than 1.6 $\mu C.\mu m^{-2}$ were much larger in diameter and consequently, more fragile mechanically. As presented in Fig.3A, the H_2O_2 - oxidation wave could be detected at the same half-wave or plateau potential with all platinized arrays, though major differences were detected concerning the amplitudes of the background/capacitive and faradaic currents of the voltammograms. Both contributions to the whole current were analyzed (Fig. 3B) as function of the array-platinization charge: capacitive currents were assimilated to the background currents and measured in PBS at +75 mV (no faradaic response), while the faradaic plateau currents were measured following a subtraction of that background current in PBS.

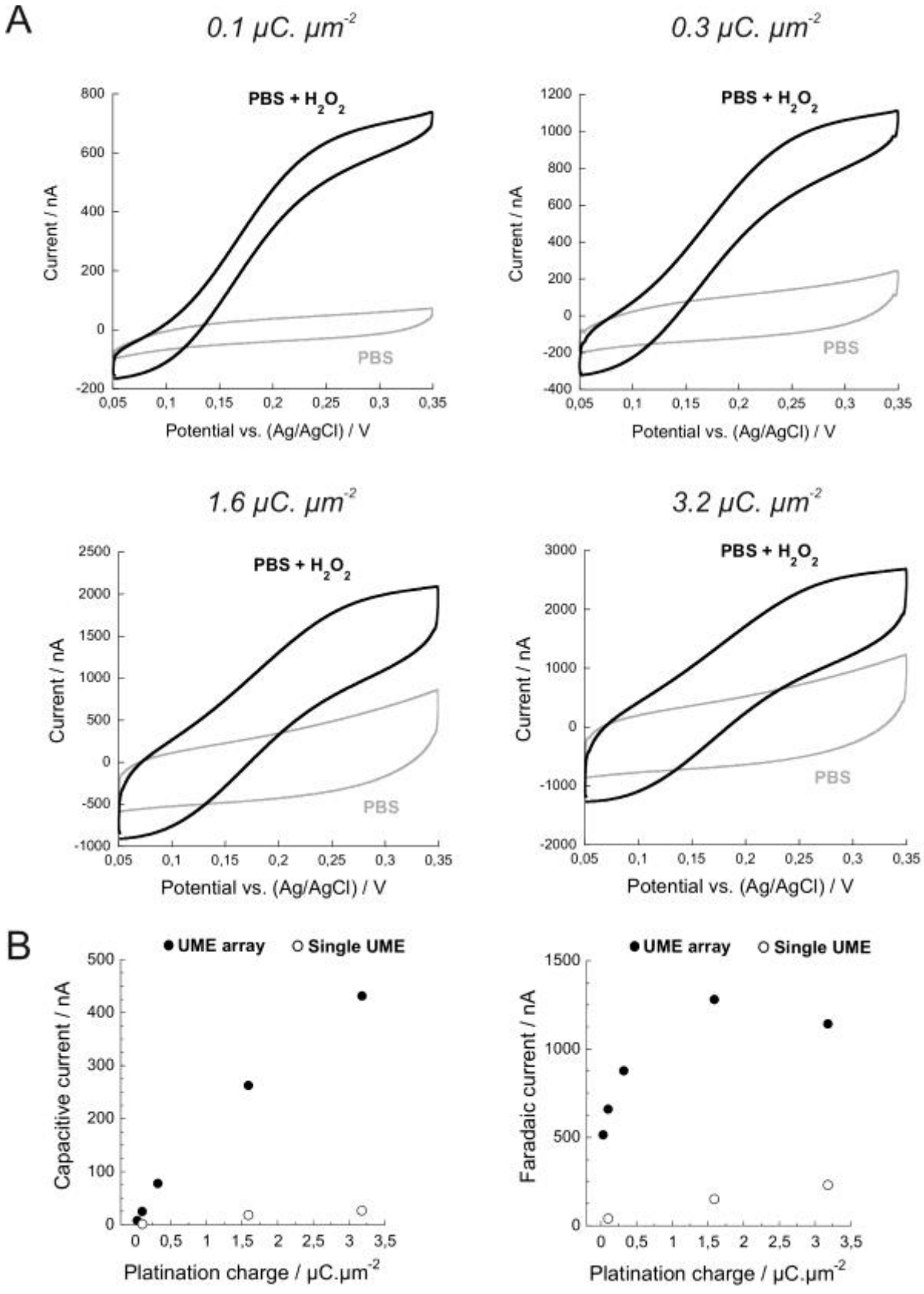
A
0.1 µC. µm-2
0.3 µC. µm-2
1.6 µC. µm-2
3.2 µC. µm-2
PBS + H2O2
PBS
Current / nA
Potential vs. (Ag/AgCl) / V
B
UME array
Single UME
Capacitive current / nA
Faradaic current / nA
Platination charge / µC.µm-2

Fig. 3. A. Cyclic voltammograms (20 $mV.s^{-1}$) recorded in a 10 mM-hydrogen peroxide solution in PBS with ultramicroelectrode arrays (16 x 20 µm-diameter platinum disk UME) platinized at different coulometric charges. B. Plots of the variation of capacitive and faradaic currents contributing to the oxidation wave of H_2O_2 10 mM as function of the coulometric charge of black-platinum electrodeposition on the arrays (black circles). The capacitive and faradaic currents detected in the same conditions on single UMEs (20µm-diameter) platinized at different charges are also reported (open circles) for comparison [24].

Results show that both currents do not follow the same trend (Fig. 3B). The capacitive current increases significantly, almost linearly, with the quantity of black-platinum electrodeposited on the array (Fig. 3B left). This evolution can be seen as an indirect measurement of the active surface increase upon the increase of the platinization coulometric charge, though the capacitance of the surface may also vary under the increase of the active surface area. Large capacitive currents are inherent to rough surfaces such as black-platinum deposits, they could be diminished when the scan rate was lowered to 5-10 $mV.s^{-1}$ in voltammetry, but they could not be discarded. Otherwise, we observe that the faradaic currents due to H_2O_2 oxidation increases with the electro-deposition charge until a maximum value of 1.6 $\mu C.\mu m^{-2}$. The faradaic response does not increase at a higher charge value, while the capacitive current increases, possibly showing that though the dimensions (volume) of the black-platinum deposit are larger, the active surface area accessible to H_2O_2 molecules remains quite constant. In addition, well-defined voltammograms with a low background-capacitive contribution were detected at lower values, e.g. 0.1 $\mu C.\mu m^{-2}$ and 0.3 $\mu C.\mu m^{-2}$ platinization charges (Fig. 3A). In comparison with the faradaic responses detected at single platinized UMEs, the ones detected on the arrays platinized

at the same charge values (from 0.1 $\mu C.\mu m^{-2}$ to 1.6 $\mu C.\mu m^{-2}$) were 14 to 9-fold higher (Fig. 3B). This ratio decreased at higher electro-deposition charges, showing that an optimum can be found at lower values taking into account the balance between the increases of both faradaic and capacitive currents due to the number of UME interconnected and the true increase of the active surface for the oxidation of H_2O_2 molecules at each UME. This latter might also depend on the exact addition or inter-penetration of spherical diffusion fields at each UME on the array, especially when large deposits are used.

Overall, this set of results show that the platinization of ultramicroelectrode arrays provides an increase of faradaic responses and consequently a better sensitivity for the detection of redox species such like ferricyanide or hydrogen peroxide, while enabling an adjustment of the platinization level to reach an optimal sensitivity and being less dependent on defaults inherent to nano-structured rough surfaces such as black-platinum.

3.3. Chrono-amperometric studies of ultramicroelectrode arrays sensitivity for hydrogen peroxide

The sensitivity and repeatability of hydrogen peroxide detection by the platinized ultramicroelectrode arrays were then assessed by chrono-amperometry at a fixed potential of +300 mV vs. Ag/AgCl (Fig. 4), corresponding to the plateau potential determined above by voltammetry. Each UME array was let to stabilize in current until reaching a drift over 10 minutes lower than 5 % of the stationary current. Then, H_2O_2 solutions were injected in the chamber containing PBS under constant stirring (conditions adequate for measurements on biological samples) to obtain, successively and several times, concentration variations of 10 nM,

100 nM, 1 µM or 10 µM. In excellent agreement with the results obtained by voltammetric measurements, the amplitude of current variations following H_2O_2 injections were dependent on the coulometric charge, and consequently, on the quantity of black-platinum electrodeposited on the array. In other words, currents detected on UME arrays platinized at 1.6 $\mu C.\mu m^{-2}$ were higher than those detected at 0.3 $\mu C.\mu m^{-2}$, which were higher to the ones obtained at 0.1. $\mu C.\mu m^{-2}$. However, it appeared that for the lowest concentrations of H_2O_2 measured, i.e. below 1 µM, sensitivity and limit of detection did not follow that trend. Because of the increase of mean noise level for more platinized UME arrays (inset in Fig. 4), the experimental limits of detection (minimum measurable concentration based on a current increase $\geq$ 3 x *rms* noise amplitude) were inversely proportional to the platinization degree; they were measured as 10 nM (noise amplitude: 5 pA), 30 nM (noise amplitude : 20 pA) and 50 nM (noise amplitude : 80 pA) for the 0.1. $\mu C.\mu m^{-2}$, 0.3 $\mu C.\mu m^{-2}$ and 1.6 $\mu C.\mu m^{-2}$ -platinized arrays, respectively. Again, this is in agreement with the voltammetric results (see 3.2. section), which showed a major increase of capacitance of black-platinum surfaces under the increase of deposition charge. Though platinized arrays were let to stabilize in current for long periods, at least 1 hour, the more platinized surfaces very susceptible to continuous capacitive current discharges. The equivalent RC filter of the electrode interface surely became a limiting factor leading to a higher noise level in amperometric measurements and a lower current stability in the sub-nanoampere range.

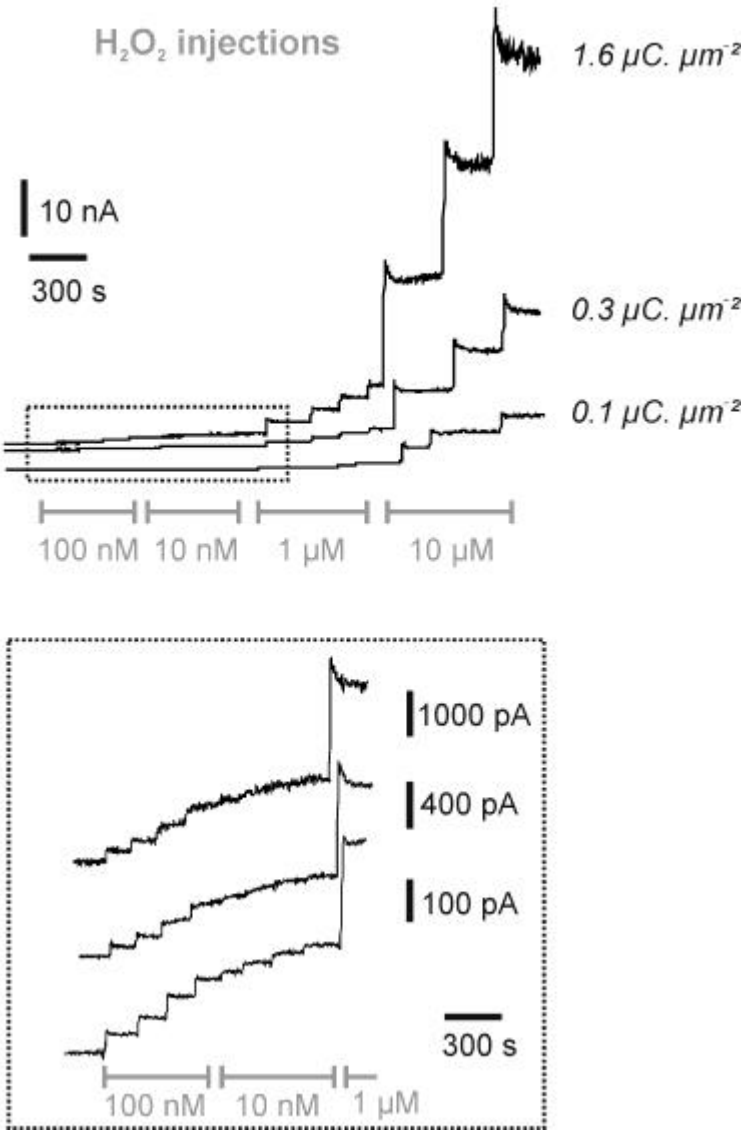

Fig. 4. Chrono-amperometric detection (E = +300 mV *vs*. Ag/AgCl) of hydrogen peroxide solutions with ultramicroelectrode arrays (16 x 20µm-diameter platinum UME) platinized at three different coulometric charges (see Fig. 3 for values). Solutions of H_2O_2 were injected in the chamber to provide successively and repeatedly concentration differences of 10 nM, 100 nM, 1 µM and 10 µM, in order to assess for the sensitivity and repeatability of response of each array. The inset shows their responses at the lowest concentrations of H_2O_2, graphs being scaled-up for a better comparison of array sensitivities.

Based on the array responses measured for the different H_2O_2 concentrations, we defined calibration curve plots (Fig. 5). We observed linear evolutions ($R^2 \geq 0.99$) of the currents detected at the arrays within the large concentration range studied herein: 10 nM – 40 µM. This range could be expanded to higher concentrations, however we focused on a concentration range corresponding to the one described for measurements in biological conditions. Moreover, the main analytical feature, sought for such sensor applied to the monitoring of biological H_2O_2, is its linearity of response since *in vivo* or *ex vivo* local concentrations may vary much as function of oxygen metabolism of involved biological entities [2, 39, 40]. This goal was clearly achieved with black-platinum modified UME arrays.

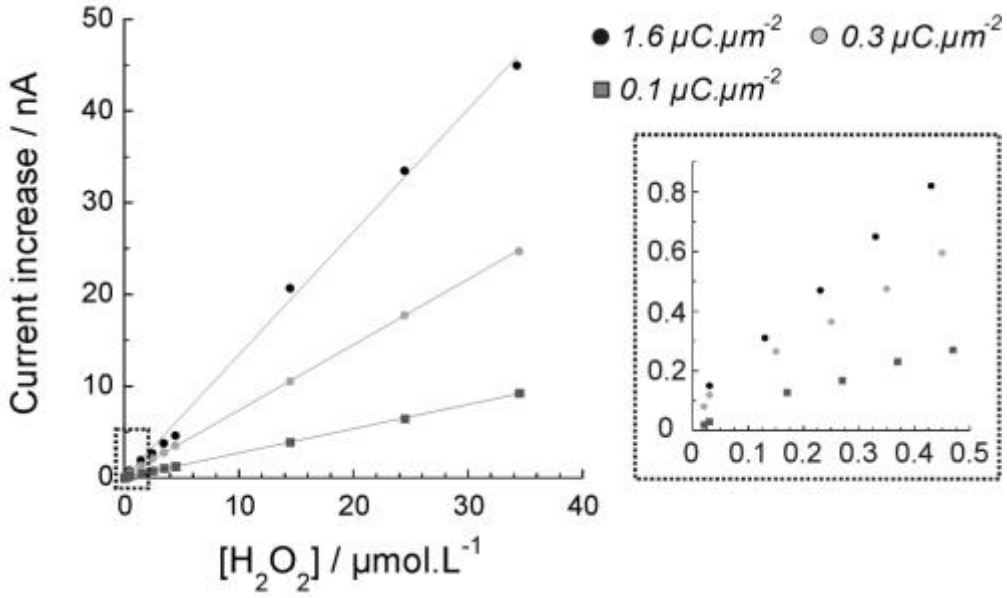

Fig. 5. Calibration curves of the amperometric responses detected with platinized-ultramicroelectrode arrays (16 x 20µm-diameter platinum UME; coulometric charges of the black-platinum electrodeposition were defined from Figures 3 and 4) versus the concentration of

H_2O_2 solutions. Inset shows values for the sub-micromolar domain of H_2O_2 concentrations. Each calibration plot, obtained from 2-3 different UME array at each condition, was fitted with a linear curve ($R^2 \geq 0.99$ in each case). All detections were achieved at +300 mV *vs*. Ag/AgCl.

3.4. Chrono-amperometric monitoring with ultramicroelectrode arrays of hydrogen peroxide produced by mitochondria

Platinized carbon or platinum ultramicroelectrodes have been used previously to monitor hydrogen peroxide releases by single living cells. [41-44] In the present study, the aim was to measure such production by sub-cellular structures, namely mitochondria. Measurements were conducted in bulk condition that is on mitochondria in suspension as achieved typically in oxygraphy measurements. Consequently, we cannot benefit from the confinement effect used for single cell measurement when the sensor surface is placed at micrometric distance from the biological source. Hydrogen peroxide concentrations due to the mitochondrial production are then homogenised in the oxygraphy chamber (V = 6 mL) and might be lower than for cells, as we and others reported recently [24, 36]. This requires highly sensitive and selective electrodes.

The above results *in vitro* showed that the sub-micromolar range of H_2O_2 concentrations could be monitored with high accuracy (10 nM limit of detection) owing to the platinized ultramicroelectrode arrays. The selectivity for H_2O_2 was checked by analysing responses of UME arrays during injections of substrates (ethanol, adenosine-diphosphate) or inhibitor (antimycin A) of mitochondrial respiration. As can be observed on the chrono-amperogram in Fig. 6, these compounds did not induce any significant faradic response apart from injection artifacts. This allowed monitoring the release of hydrogen peroxide by model mitochondria,

extracted from yeasts *Saccharomyces cerevisiae*. Hydrogen peroxide and its mother species superoxide radical anion (reactive oxygen species: ROS) are by-products of the respiratory chain activity in mitochondria. They are harmful for biological systems but also have been shown to be involved in intracellular signalling. Measuring such production in different activation or inhibitory conditions is thus of major interest for understanding these signalling pathways [3, 40, 45].

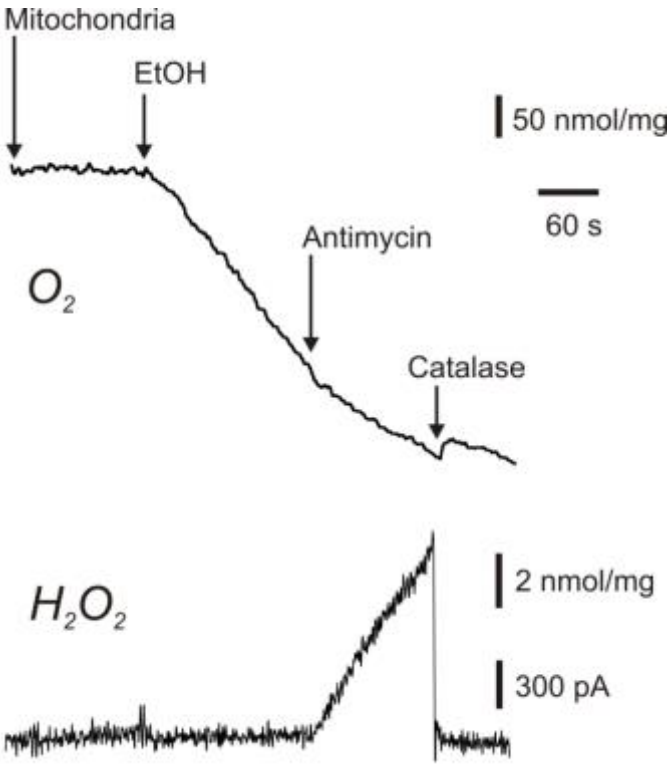

Fig. 6. Chrono-amperometric monitoring (+300 mV vs. Ag/AgCl) with a platinized ultramicroelectrode array (coulometric charge of platinization : 1.6 $\mu C.\mu m^{-2}$) of hydrogen peroxide production by mitochondria, in conjunction with the measurement of their oxygen consumption by a Clark macroelectrode (-850 mV vs. Ag/AgCl). Mitochondria (0.45 mg/mL), which intrinsic catalase activity was previously inhibited (see experimental section), were first

injected in the analysis chamber containing the aerated "respiratory" buffer (T 28°C), and then energized by ethanol (1% final concentration). Following, the respiratory chain was inhibited by adding Antimycin A (0.5 µM final concentration). Finally, the nature of the H_2O_2 signal was confirmed by injecting exogenous catalase (400 u/mL).

Herein, mitochondria were injected in the analysis chamber and rapidly activated, namely energized, by the addition of ethanol. Ethanol and NAD^+ are converted in yeast mitochondria by alcohol dehydrogenase into acetaldehyde and NADH, which is the initial substrate of NADH dehydrogenase in the respiratory chain. In that condition, the production of ROS (often considered as a "leakage" of electrons from the respiratory chain) is negligible as compared to oxygen consumption by mitochondria as observed on Fig. 6. The production of ROS, and consequently the release of hydrogen peroxide by mitochondria is obtained by inhibiting the respiratory activity. This was achieved by injecting Antimycin A, a well-known inhibitor of complex III. Thus, electrons are no longer transferred to cytochrome c oxidase (complex IV), but indirectly to oxygen via an ubiquinone reactive intermediate. In the seconds following injection of Antimycin A, the chrono-amperometric current increased. Current rose linearly, as expected from the change of slope of respiratory rate (top curve Fig. 6), and reached with a 1.6 $\mu C.\mu m^{-2}$ platinized array, a level that is 1200 pA above the initial current level (energized state). This allowed calculating a mean flux of 1 nanomole/min./mg protein for H_2O_2 production. Actually, we injected exogenous catalase within the chamber to decompose H_2O_2 and check out for selectivity. The current rapidly returned to the baseline level, showing that the signal could be fully attributed to hydrogen peroxide oxidation.

In addition, these data demonstrate the necessity of developing electrochemical sensors for H_2O_2 in the sub-micromolar concentration domain. The H_2O_2 flux detected on mitochondria could not be detected on bare platinum electrodes. Surface features of black platinum-modified UME arrays enabled reaching a limit of detection and sensitivity in agreement with the fluxes of H_2O_2 produced and released by mitochondria.

CONCLUSIONS

There is a major interest for biomedical studies to detect quantitatively hydrogen peroxide in the micro to nano-molar concentration range. We demonstrated herein that platinized ultramicroelectrode arrays match this requirement and represent a clear improvement over a single platinized UME. Indeed, while still being small enough to be used for local measurements such as for in vivo detection, they provide much larger current and better sensitivity than a single electrode. We showed that an H_2O_2 concentration as low as 10 nM was detected in physiological condition, with a response-time of 1 sec. at most. In addition, the microchips developed herein integrate several UME arrays, which could be used in parallel to monitor several species of interest following possibly a different surface functionalization of each array. This opens the way for numerous biological applications, such like multi-parametric studies of mitochondrial activities in different physio-pathological conditions.

ACKNOWLEDGMENT

The project was financially supported by the University of Bordeaux, the CNRS (“Centre National de la Recherche Scientifique “; UMR 5255, UPR 8001 and UMR 5095; ATIP grant for SA), and the ANR (“Agence Nationale pour la Recherche”, NANOMITO project

n°ANR2011BSV502501). The technological realizations and associated research works were partly supported by the French RENATECH network. Aurélie Ladonne is acknowledged for help during yeast culture and mitochondria preparations.

REFERENCES

[1] B. D'Autreaux, M.B. Toledano, Nat. Rev. Mol. Cell Biol., 8 (2007) 813-824.

[2] D.R. Gough, T.G. Cotter, Cell Death Dis., 2 (2011) e213.

[3] M. Rigoulet, E.D. Yoboue, A. Devin, Antioxid. Redox Signal., 14 (2011) 459-468.

[4] W. Chen, S. Cai, Q.Q. Ren, W. Wen, Y.D. Zhao, Analyst, 137 (2012) 49-58.

[5] M. Schaferling, D.B.M. Grogel, S. Schreml, Microchim. Acta, 174 (2011) 1-18.

[6] T. Gan, S.S. Hu, Microchim. Acta, 175 (2011) 1-19.

[7] A.A. Karyakin, E.A. Kuritsyna, E.E. Karyakina, V.L. Sukhanov, Electrochim. Acta, 54 (2009) 5048-5052.

[8] P.A. Prakash, U. Yogeswaran, S.M. Chen, Sensors, 9 (2009) 1821-1844.

[9] D.W. Kimmel, G. LeBlanc, M.E. Meschievitz, D.E. Cliffel, Anal. Chem., 84 (2012) 685-707.

[10] S.A.G. Evans, J.M. Elliott, L.M. Andrews, P.N. Bartlett, P.J. Doyle, G. Denuault, Anal. Chem., 74 (2002) 1322-1326.

[11] B.D. Pacheco, J. Valerio, L. Angnes, J.J. Pedrotti, Anal. Chim. Acta, 696 (2011) 53-58.

[12] S.H. Chen, R. Yuan, Y.Q. Chai, F.X. Hu, Microchim. Acta, 180 (2013) 15-32.

[13] P. Karam, L.I. Halaoui, Anal. Chem., 80 (2008) 5441-5448.

[14] A.A. Karyakin, E.A. Puganova, I.A. Budashov, I.N. Kurochkin, E.E. Karyakina, V.A. Levchenko, V.N. Matveyenko, S.D. Varfolomeyev, Anal. Chem., 76 (2004) 474-478.

[15] H.A. Zhong, R. Yuan, Y.Q. Chai, Y. Zhang, C.Y. Wang, F. Jia, Microchim. Acta, 176 (2012) 389-395.

[16] C. Amatore, S. Arbault, Y. Bouret, B. Cauli, M. Guille, A. Rancillac, J. Rossier, ChemPhysChem, 7 (2006) 181-187.

[17] C. Amatore, S. Arbault, A.C.W. Koh, Anal. Chem., 82 (2010) 1411-1419.

[18] P.M. Talauliker, D.A. Price, J.J. Burmeister, S. Nagari, J.E. Quintero, F. Pomerleau, P. Huettl, J.T. Hastings, G.A. Gerhardt, J. Neurosci. Meth., 198 (2011) 222-229.

[19] O. Niwa, T. Horiuchi, M. Morita, T.H. Huang, P.T. Kissinger, Anal. Chim. Acta, 318 (1996) 167-173.

[20] T.W. Sohn, P.W. Stoecker, W. Carp, A.M. Yacynych, Electroanal., 3 (1991) 763-766.

[21] S. Arbault, P. Pantano, J.A. Jankowski, M. Vuillaume, C. Amatore, Anal. Chem., 67 (1995) 3382-3390.

[22] A. Rancillac, J. Rossier, M. Guille, X.K. Tong, H. Geoffroy, C. Amatore, S. Arbault, E. Hamel, B. Cauli, J. Neurosci., 26 (2006) 6997-7006.

[23] Y. Ikariyama, S. Yamauchi, T. Yukiashi, H. Ushioda, Anal. Lett., 20 (1987) 1407-1416.

[24] S. Ben-Amor, A. Devin, M. Rigoulet, N. Sojic, S. Arbault, Electroanal., 25 (2013) 656-663.

[25] Y. Li, C. Sella, F. Lemaitre, M.G. Collignon, L. Thouin, C. Amatore, Electroanal., 25 (2013) 895-902.

[26] K. Aoki, Electroanal., 5 (1993) 627-639.

[27] O. Ordeig, J. del Campo, F.X. Munoz, C.E. Banks, R.G. Compton, Electroanal., 19 (2007) 1973-1986.

[28] M.E. Sandison, N. Anicet, A. Glidle, J.M. Cooper, Anal. Chem., 74 (2002) 5717-5725.

[29] K. Dawson, J. Strutwolf, K.P. Rodgers, G. Herzog, D.W.M. Arrigan, A.J. Quinn, A. O'Riordan, Anal. Chem., 83 (2011) 5535-5540.

[30] M. Delvaux, A. Walcarius, S. Demoustier-Champagne, Anal. Chim. Acta, 525 (2004) 221-230.

[31] A. Lupu, P. Lisboa, A. Valsesia, P. Colpo, F. Rossi, Sensor. Actuat. B-Chem., 137 (2009) 56-61.

[32] C. Christophe, F.S. Belaidi, J. Launay, P. Gros, E. Questel, P. Temple-Boyer, Sensor. Actuat. B-Chem., 177 (2013) 350-356.

[33] E. Vanhove, A. Tsopela, L. Bouscayrol, A. Desmoulin, J. Launay, P. Temple-Boyer, Sensor. Actuat. B-Chem., 178 (2013) 350-358.

[34] J. Velours, B. Guerin, M. Duvert, Arch. Biochem. Biophys., 182 (1977) 295-304.

[35] M. Salvi, V. Battaglia, A.M. Brunati, N. La Rocca, E. Tibaldi, P. Pietrangeli, L. Marcocci, B. Mondovi, C.A. Rossi, A. Toninello, J. Biol. Chem., 282 (2007) 24407-24415.

[36] R. Marcu, S. Rapino, M. Trinei, G. Valenti, M. Marcaccio, P.G. Pelicci, F. Paolucci, M. Giorgio, Bioelectrochem., 85 (2012) 21-28.

[37] A. Kicela, S. Daniele, Talanta, 68 (2006) 1632-1639.

[38] J.S. Mayell, J. Electrochem. Soc., 113 (1966) 385-&.

[39] G.J. Maghzal, K.H. Krause, R. Stocker, V. Jaquet, Free Radic. Biol. Med., 53 (2012) 1903-1918.

[40] P. Venditti, L. Di Stefano, S. Di Meo, Mitochondrion, 13 (2013) 71-82.

[41] S. Arbault, P. Pantano, N. Sojic, C. Amatore, M. BestBelpomme, A. Sarasin, M. Vuillaume, Carcinogenesis, 18 (1997) 569-574.

[42] S. Arbault, N. Sojic, D. Bruce, C. Amatore, A. Sarasin, M. Vuillaume, Carcinogenesis, 25 (2004) 509-515.

[43] C. Amatore, S. Arbault, D. Bruce, P. de Oliveira, M. Erard, M. Vuillaume, Farad. Discuss., 116 (2000) 319-333.

[44] S. Bergner, J. Wegener, F.M. Matysik, Anal. Chem., 83 (2011) 169-174.

[45] S. Bolisetty, E.A. Jaimes, Int. J. Mol. Sci., 14 (2013) 6306-6344.